Development 138, 4931-4942 (2011) doi:10.1242/dev.066597

HESX1- and TCF3-mediated repression of Wnt/β-catenin targets is required for normal development of the anterior forebrain

Cynthia L. Andoniadou*,[1], Massimo Signore*,[1], Rodrigo M. Young[2], Carles Gaston-Massuet[1], Stephen W. Wilson[2], Elaine Fuchs[3] and Juan Pedro Martinez-Barbera[1,‡]

SUMMARY

The Wnt/β-catenin pathway plays an essential role during regionalisation of the vertebrate neural plate and its inhibition in the most anterior neural ectoderm is required for normal forebrain development. *Hesx1* is a conserved vertebrate-specific transcription factor that is required for forebrain development in *Xenopus*, mice and humans. Mouse embryos deficient for *Hesx1* exhibit a variable degree of forebrain defects, but the molecular mechanisms underlying these defects are not fully understood. Here, we show that injection of a *hesx1* morpholino into a 'sensitised' zygotic *headless* (*tcf3*) mutant background leads to severe forebrain and eye defects, suggesting an interaction between Hesx1 and the Wnt pathway during zebrafish forebrain development. Consistent with a requirement for Wnt signalling repression, we highlight a synergistic gene dosage-dependent interaction between *Hesx1* and *Tcf3*, a transcriptional repressor of Wnt target genes, to maintain anterior forebrain identity during mouse embryogenesis. In addition, we reveal that *Tcf3* is essential within the neural ectoderm to maintain anterior character and that its interaction with *Hesx1* ensures the repression of Wnt targets in the developing forebrain. By employing a conditional loss-of-function approach in mouse, we demonstrate that deletion of β-catenin, and concomitant reduction of Wnt signalling in the developing anterior forebrain of *Hesx1*-deficient embryos, leads to a significant rescue of the forebrain defects. Finally, transcriptional profiling of anterior forebrain precursors from mouse embryos expressing *eGFP* from the *Hesx1* locus provides molecular evidence supporting a novel function of *Hesx1* in mediating repression of Wnt/β-catenin target activation in the developing forebrain.

KEY WORDS: *Hesx1*, *Tcf3* (*Tcf7l1*), Wnt/β-catenin, Forebrain, Mouse, Zebrafish

INTRODUCTION

Suppression of posteriorising signals, and in particular of Wnt signalling, is necessary for correct forebrain specification (Buchert et al., 2010; Felix and Aboobaker, 2010; Fredieu et al., 1997; Heisenberg et al., 2001; Houart et al., 2002; Kimura et al., 2000; Kudoh et al., 2002; Perea-Gomez et al., 2001; van de Water et al., 2001; Wilson and Houart, 2004). Inhibitors that are able to sequester Wnt molecules or to bind their receptors are secreted either locally within the neuroectoderm (Houart et al., 2002) or from underlying tissues (Glinka et al., 1997; Kazanskaya et al., 2000; Piccolo et al., 1999) to abolish Wnt signalling in the forebrain. In addition, other molecules act within the receiving cell to either bind to β-catenin (Garaventa et al., 1999; Satoh et al., 2004) or to interfere with receptor maturation (Yamamoto et al., 2005) to ensure that the pathway is inactive within the anterior neural plate. The combination of these cell- and non-cell-autonomous mechanisms is thought to lead to the establishment of a high-posterior to low-anterior gradient of Wnt signalling that provides the positional information required for the regionalisation of the incipient neural plate into the fore, mid and hindbrain. However, less is known about how Wnt/β-catenin target genes are repressed in forebrain precursors.

β-catenin, the product of *Ctnnb1*, is at the centre of the canonical Wnt pathway. In the absence of Wnt molecules, β-catenin is phosphorylated by a 'destruction complex' formed by several proteins, including GSK3β, CK1α, AXIN1 and APC, and targeted for ubiquitylation and subsequent proteasome-mediated degradation. Binding of secreted Wnt ligands to Frizzled and LRP membrane receptors causes the disassembly of the destruction complex and inhibition of β-catenin phosphorylation. This results in the cytoplasmic accumulation of β-catenin, which can enter the nucleus to interact with DNA-binding TCF/LEF transcription factors and activate transcription of Wnt target genes (reviewed by van Amerongen and Nusse, 2009).

Among the four TCF/LEF factor family members, only *Tcf3* (*Tcf7l1*) is expressed in the developing forebrain primordium of the mouse at presomitic and early somite stages (Galceran et al., 1999; Merrill et al., 2004). Experiments in *Xenopus laevis* indicate that *tcf3* acts as a repressor of Wnt targets and interacts with Groucho co-repressors (Brannon et al., 1999; Brantjes et al., 2001; Houston et al., 2002). In zebrafish, knockdown of both paralogues of *Tcf3*, *tcf3a* (*tcf7l1a*) and *tcf3b* (*tcf7l1b*), results in loss of repressor activity and in anterior truncations (Kim et al., 2000), indicating that there is a requirement for the β-catenin-independent Tcf repressor activity in head morphogenesis (Dorsky et al., 2003). In mouse, *Tcf3*-deficient embryos undergo gastrulation but exhibit variable degrees of defects, including primitive streak and axis duplications, supernumerary neural folds, and neural patterning defects involving expansion of

[1]Neural Development Unit, UCL Institute of Child Health, 30 Guilford Street, London WC1N 1EH, UK. [2]Department of Cell and Developmental Biology, UCL, Gower Street, London WC1E 6BT, UK. [3]Howard Hughes Medical Institute, Laboratory of Mammalian Cell Biology & Development, The Rockefeller University, New York, NY 10065, USA.

*These authors contributed equally to this work
‡Author for correspondence (j.martinez-barbera@ich.ucl.ac.uk)

Accepted 8 September 2011

midbrain at the expense of forebrain and hindbrain tissues (Merrill et al., 2004). However, the mechanisms underlying these defects are not fully understood because *Tcf3* is expressed prior to the onset of gastrulation in the epiblast, anterior mesendoderm and anterior neuroectoderm, and defects in any of these could lead to aberrant neural patterning. Specifically, whether *Tcf3* plays a role within forebrain tissue remains unknown (Merrill et al., 2004).

HESX1 is a paired-like homeobox transcription factor that is expressed in the anterior regions of the vertebrate embryo but is absent from invertebrates, including close relatives such as ascidians, amphioxus and *Ciona intestinalis* (Kazanskaya et al., 1997; Martinez-Barbera et al., 2000). Using genetic fate mapping, we have previously shown that derivatives of *Hesx1*-expressing precursors that are normally destined to populate the anterior forebrain (cerebral cortex, basal ganglia, ventral diencephalon and eyes) change their fate in *Hesx1*-deficient embryos and colonise posterior forebrain regions as well as the neural crest lineage (Andoniadou et al., 2007). A similar posterior transformation of anterior forebrain is observed in knockdown experiments of the *Hesx1* orthologue *Xanf* in *Xenopus* (Ermakova et al., 1999). The molecular mechanisms responsible for the lack of anterior identity and cell fate transformation are not known. Understanding the pathogenesis of these early defects is also of clinical relevance, as mutations in *HESX1* result in forebrain, eye and pituitary defects in humans (Dattani et al., 1998; Sajedi et al., 2008).

In this study we sought to specifically address the molecular function of *Hesx1* in anterior forebrain precursors. Combining genetic and molecular approaches we reveal a novel role for *Hesx1* as an antagonist of the Wnt/β-catenin pathway in the mouse and zebrafish forebrain. In addition, we demonstrate a requirement for *Tcf3* in forebrain progenitors, where it genetically interacts with *Hesx1* to promote anterior character by repressing the transcriptional activation of Wnt/β-catenin target genes.

MATERIALS AND METHODS

Animals

Wild-type and *zhdl*^{m881} zebrafish embryos were raised at 28°C and staged according to Kimmel et al. (Kimmel et al., 1995). Single-cell embryos were injected with 5 nl of 0.5 pmol/nl *hesx1* morpholino (5′-TGCAAGAGAAGCCATTGCTAAACTC-3′, GeneTools) and/or 1 pg/nl mouse *Hesx1* mRNA. *hdl*^{m881} mutant embryos were genotyped as described (Kim et al., 2000).

Hesx1-Cre, *Ctnnb1-lox(ex2-6)*, *Tcf3-flox*, *R26-YFP*, *BAT-gal*, *Six3-lacZ*, *Hesx1*$^{+/-}$ and *Ctnnb1*$^{+/-}$ mice have been described previously (Andoniadou et al., 2007; Brault et al., 2001; Lagutin et al., 2003; Maretto et al., 2003; Nguyen et al., 2009; Srinivas et al., 2001; Dattani et al., 1998; Haegel et al., 1995). *Tcf3*$^{fl/+}$ animals were crossed with the *Actb-Cre* strain to generate *Tcf3*$^{+/-}$ animals, which were bred further on C57BL/6 in order to remove the *Cre* transgene from the background. Breeding of genetically modified animals and all animal procedures were carried out under the UK Home Office Animals (Scientific Procedures) Act 1986. A mixed background, backcrossed onto C57BL/6, was used for all strains. Embryos and pups were genotyped by PCR on DNA from yolk sacs, tail buds or ear biopsies as described previously (Andoniadou et al., 2007). Briefly, the thermal profile comprised a single step for 2 minutes at 94°C, followed by 35 cycles of 94°C for 30 seconds, 60°C for 30 seconds and 72°C for 45 seconds. The wild-type and mutant alleles yield bands of ~500 bp and 250 bp, respectively. For primers, see supplementary material Table S9.

The Hesx1-eGFP targeting vector was generated using homologous regions obtained from plasmids carrying the mouse *Hesx1* gene (Dattani et al., 1998). A cassette containing eGFP followed by (1) four SV40 and one PGK polyadenylation sites flanked by *loxP* sequences, (2) the diphtheria toxin A (DTA) coding sequence (Ivanova et al., 2005) and (3) a PGK-Neo cassette flanked by frt sequences (Andoniadou et al., 2007) was cloned into a vector containing ~6.5 kb and 1.3 kb of 5′ and 3′ homologous regions, respectively (Fig. 5). The linearised targeting vector was electroporated into CCE ES cells (129/SvEv; kindly provided by E. Robertson, Sir William Dunn School of Pathology, Oxford, UK) and ~400 colonies were picked, expanded and screened by PCR and Southern blot, as described previously (Andoniadou et al., 2007). Two correctly targeted clones were isolated and injected into blastocysts from C57BL/6J (Harlan) mice. Male chimeras were backcrossed to C57BL/6J females to establish the F1 generation of heterozygous mice. F1 animals were crossed to the *Actb:FLPe* strain (Rodriguez et al., 2000), kept on a C57BL/6J background, to excise the PGK-Neo cassette. After backcrossing with C57BL/6J animals to remove the *FLPe* transgene, *Hesx1*$^{eGFP/+}$ heterozygotes were kept on a C57BL/6J background.

Flow sorting

For microarray gene profiling, 3- to 5-somite embryos from *Hesx1*$^{eGFP/+}$ intercrosses were selected for eGFP expression, phenotyped and grouped into normal (*Hesx1*$^{eGFP/+}$) and mutant (*Hesx1*$^{eGFP/eGFP}$). Pieces of each embryo were retained for genotyping to ensure the integrity of each pool. Embryos were manually dissociated, and single cells were flow sorted using a MoFlo XDP (Beckman Coulter, Fullerton, CA, USA) directly into Buffer RLT (Qiagen) for RNA extraction. Fluorescence was detected using a 530/540 filter. Cell sorting data were analysed using Summit software (Dako).

Microarray analysis

Total RNA was isolated using the RNeasy Micro Kit (Qiagen) according to the manufacturer's recommendations with the addition to the lysis buffer of 500 ng bacterial ribosomal RNA (Roche) per reaction as carrier. cDNA synthesis, linear amplification and labelling of cRNA were carried out according to the manufacturer's protocols using the GeneChip 3′ IVT Express Kit (Affymetrix). Gene expression profiling was performed to compare eGFP-positive purified anterior forebrain precursors from *Hesx1*$^{eGFP/+}$ (normal) and *Hesx1*$^{eGFP/eGFP}$ embryos on the Affymetrix Mouse430_2 platform using the GeneChip Hybridisation, Wash and Stain Kit (Affymetrix). This analysis was carried out in triplicate for each genotype, over a ~1 year period, using independently isolated pools of cells from several embryos (n=20-30 for each replicate) and was validated on independent biological samples by qRT-PCR (supplementary material Fig. S3). Gene expression data are deposited at ArrayExpress with ID: E-MEXP-2586. Files were processed in MATLAB (MathWorks) and GeneSpring GX (Agilent Technologies). GC-RMA normalisation was carried out and significantly differentially expressed genes were identified after the Benjamini and Hochberg false discovery rate was applied as a multiple testing correction method. GeneSpring Gene Ontology and DAVID databases were used to generate pathway lists. Where multiple probe sets were available for a single gene, the value of the unique probe set was used, or, in the case of multiple unique probe sets, that with the highest raw intensity levels.

In situ hybridisation, immunofluorescence and X-Gal staining

Wholemount in situ hybridisation, X-Gal staining and immunofluorescence on paraffin sections were performed as previously described (Andoniadou et al., 2007). Antibodies against GFP (Invitrogen, 1:350), cleaved caspase 3 (Cell Signaling Technology, 1:200) and phospho-histone H3 (Upstate, 1:300) were detected with Alexa Fluor-conjugated secondary antibodies (Invitrogen, 1:350).

Quantitative real-time (qRT) PCR

RNA was extracted using the RNeasy Micro Kit (Qiagen) following the manufacturer's protocols and including on-column DNaseI digestion. Up to 2 μg RNA was used for cDNA synthesis using Omniscript reverse transcriptase (Qiagen) with random hexamers (Promega).

qRT-PCR was carried out to validate microarray results, on independent biological replicates in triplicate. Briefly, 10-50 ng template cDNA was used per reaction on an ABI 7500 Fast Cycler employing SYBR-based technology using MESA Blue reagent (Eurogentec) and specific primers (supplementary material Table S10). The thermal profile comprised a single step for 2 minutes at 50°C to activate UNG (uracil-N-glycosylase) and destroy contaminating uracil-containing template, followed by 10 minutes at 95°C

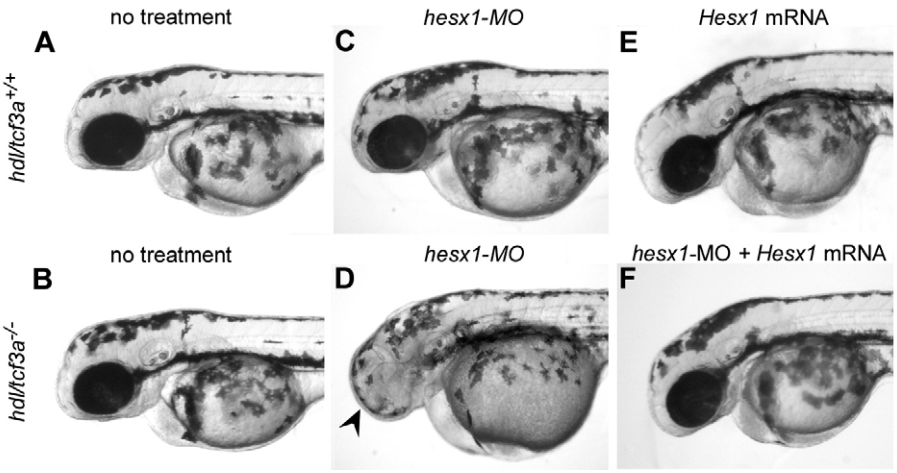

Fig. 1. *hesx1* and *hdl* (*tcf3a*) genetically interact for proper anterior-posterior patterning of the zebrafish brain. Lateral views of 2 day post-fertilisation zebrafish embryos. (**A**,**B**) Untreated embryos of $hdl^{+/-}$ control (A) and $hdl^{-/-}$ (B) genotypes, both showing normal forebrain development. (**C**,**D**) Injection with zebrafish *hesx1* MO at the one-cell stage to knockdown Hesx1 results in anterior defects in $hdl^{-/-}$ embryos (arrowhead in D), which are sensitised to increased levels of Wnt signalling. Injection of *hesx1* MO into control $hdl^{+/-}$ embryos has no effect (C). (**E**,**F**) Anterior defects generated by *hesx1* MO injection are rescued by co-injection of murine *Hesx1* mRNA (F). Injection of *Hesx1* mRNA alone has no effect (E).

to denature UNG and activate Taq polymerase, then 40 cycles of 95°C for 15 seconds and 60°C for 1 minute. Results were normalised to endogenous levels of *Gapdh* and were analysed using the ΔΔCt method.

We assessed excision in the forebrain by quantitative PCR on DNA using primers specifically designed against exon 3 of *Ctnnb1*, which should be excised in *Ctnnb1-lox(ex2-6)* embryos in the presence of Cre recombinase. DNA was extracted from dissected forebrains (anterior to the telencephalic/diencephalic boundary) of 9.5 dpc embryos using the DNA Micro Kit (Qiagen) using standard protocols. Primers against *Gapdh* provided an endogenous control and results were analysed using the ΔΔCt method.

Microscopy

Images of live embryos or after fixation or wholemount in situ hybridisation were captured using a Leica TCS camera and IM50 software (Leica). Images were processed using Photoshop (Adobe).

RESULTS

HESX1 can antagonise Wnt signalling, a role conserved between zebrafish and mouse

To test whether HESX1 acts to maintain anterior forebrain identity by antagonising Wnt signalling, we investigated the effect of reducing *hesx1* (previously *anf*) levels in zygotic *headless* (*hdl*; *tcf3a*, *tcf7l1a*) zebrafish mutants. The *hdl* phenotype, which results from a mutation in one of the two zebrafish *tcf3* paralogues, was initially characterised as a maternal zygotic (mz) mutant that displayed a severe anterior truncation phenotype, including the absence of eyes (Kim et al., 2000). However, this phenotype is not observed in zygotic (z) *hdl* mutants owing to compensation by *tcf3b*, which is also expressed in the anterior neural plate of the zebrafish embryo (Dorsky et al., 2003) (Fig. 1B). Indeed, the severe *mzhdl* forebrain defects can be induced in *zhdl* mutants upon injection of *tcf3b*-specific morpholinos (MOs) (Dorsky et al., 2003). We took advantage of this 'sensitised' z*hdl* background to investigate the function of *hesx1* in zebrafish.

Injection of *hesx1* MO into wild-type embryos had no effect (Fig. 1C; 2.5 pmol/embryo, n>100). However, when we injected embryos from $hdl^{+/-}$ intercrosses, we found anterior forebrain defects in ~25% of cases, which were confirmed to be homozygous mutants by *hdl* genotyping (Table 1; Fig. 1D). No defects were induced in other genotypes. The absence of eyes was apparent in $hdl^{-/-}$ *hesx1* morphant embryos, as was the absence of the telencephalon and part of the diencephalon, indicating that the phenotype is similar to the *mzhdl* phenotype (Kim et al., 2000). This phenotype was specific to the knockdown of Hesx1, as co-injection of *hesx1* MO in embryos from $hdl^{+/-}$ intercrosses together with mouse *Hesx1* mRNA (which lacks the MO target) resulted in the complete rescue of forebrain defects of $zhdl^{-/-}$ *hesx1* morphants (Table 1; Fig. 1F). This confirms that the role of Hesx1 in the forebrain is conserved in both species.

In conclusion, these results reveal that loss of Hesx1 is capable of inducing a phenotype in $hdl^{-/-}$ embryos that is consistent with an overactivation of Wnt signalling, making it likely to act as an antagonist of the Wnt pathway. Our results also suggest that a gene interaction between *hesx1* and *tcf3* is required during normal forebrain development of the zebrafish embryo.

There is a dose-dependent genetic interaction between *Hesx1* and *Tcf3* during anterior forebrain development

To investigate whether a genetic interaction between *Hesx1* and *Tcf3* is conserved in mammals, we generated mice carrying a specific gene dosage of *Hesx1* and *Tcf3*.

$Hesx1^{Cre/+}$ heterozygous animals carry a null allele in which the gene encoding Cre recombinase replaces the entire *Hesx1* coding region. These mice are mostly normal, although there is a low (<5%) incidence of eye defects (Table 2) (Andoniadou et al., 2007). The presence of Cre is not relevant for this experiment and $Hesx1^{Cre/+}$ embryos are equivalent to $Hesx1^{+/-}$. $Tcf3^{+/-}$ mice carry a null allele and are also viable and fertile (Merrill et al., 2004). By contrast, $Hesx1^{Cre/+};Tcf3^{+/-}$ or $Hesx1^{+/-};Tcf3^{+/-}$ double-heterozygous embryos from crosses between $Hesx1^{Cre/-};Tcf3^{+/-}$ and $Hesx1^{+/-}$ showed partial penetrance and displayed a variable range of anterior defects that were classified into two categories: class I defects, where embryos

Table 1. Injection of zebrafish embryos from $hdl^{+/-}$ intercrosses with zebrafish *hesx1* MO, with or without mouse *Hesx1* mRNA

	Without eyes		Normal development		
Treatment	$hdl^{-/-}$	Other genotypes	$hdl^{-/-}$	Other genotypes	Total
hesx1 MO	18	0	0	63	81
hesx1 MO + *Hesx1* mRNA	0	0	25	55	80

Treatment was with 2.5 pmol/embryo *hesx1* MO with or without 5 pg mouse *Hesx1* mRNA.

Table 2. Genotypes of embryos from *Hesx1*$^{Cre/+}$;*Tcf3*$^{+/-}$ × *Hesx1*$^{+/-}$ crosses, classified according to severity of anterior defects

		Class of forebrain defects				
Genotype	Number of embryos	None	I	II	III	IV
Hesx1$^{+/+}$;*Tcf3*$^{+/+}$	24	24	–	–	–	–
Hesx1$^{+/-}$;*Tcf3*$^{+/+}$	27	27	–	–	–	–
Hesx1$^{Cre/+}$;*Tcf3*$^{+/+}$	20	19	1	–	–	–
Hesx1$^{Cre/+}$;*Tcf3*$^{+/-}$	22	4	9	9	–	–
Hesx1$^{+/-}$;*Tcf3*$^{+/-}$	11	4	2	5	–	–
Hesx1$^{Cre/-}$;*Tcf3*$^{+/+}$	24	–	–	11	13	–
Hesx1$^{Cre/-}$;*Tcf3*$^{+/-}$	13	–	–	–	–	13
Hesx1$^{+/+}$;*Tcf3*$^{+/-}$	20	20	–	–	–	–
Total	161					

Defects were classified as: Class I, unilateral microphthalmia with normal telencephalic vesicles; class II, bilateral microphthalmia or unilateral anophthalmia with reduction in size of the telencephalic vesicles; class III, bilateral anophthalmia with reduction in size of the telencephalic vesicles; and class 4, complete absence of anterior forebrain development.

showed only unilateral microphthalmia and the telencephalon developed normally; and class II defects, in embryos with bilateral microphthalmia and/or unilateral anophthalmia in conjunction with a reduction in size of the telencephalic vesicles (*n*=33; Table 2; supplementary material Fig. S1C-E).

In situ hybridisation for specific regional markers revealed a reduction of their expression domains concomitant with the progressive loss of anterior tissue. Expression of the forkhead box-containing transcription factor *Foxg1*, which is essential for normal development of the telencephalon, was markedly reduced only in class II embryos (*n*=5; Fig. 2E). Likewise, expression of *Fgf8*, a crucial signalling molecule during forebrain development (Meyers et al., 1998; Shimamura and Rubenstein, 1997), at the anterior tip of the telencephalon (ANR, anterior neural ridge) was reduced only in class II *Hesx1*$^{Cre/+}$;*Tcf3*$^{+/-}$ embryos (*n*=6; Fig. 2D,D′). The expression domain of *Pax6*, a paired box transcription factor involved in forebrain patterning and boundary formation, was also reduced in the telencephalon and eye of class I and II embryos but extended normally to the posterior forebrain-midbrain boundary, suggesting that more caudal regions were unaffected (*n*=7; Fig. 2F).

To reduce gene dosage further, *Hesx1*$^{Cre/-}$;*Tcf3*$^{+/-}$ embryos were generated. *Hesx*$^{Cre/-}$;*Tcf3*$^{+/+}$ embryos usually displayed a fully penetrant phenotype with variable expressivity, extending from class II to a group with more severe defects than those described above, termed class III, which include bilateral anophthalmia as well as a reduction in telencephalic tissue (Andoniadou et al., 2007) (Table 2; supplementary material Fig. S1F,G). When a copy of *Tcf3* was removed in *Hesx1*$^{Cre/-}$;*Tcf3*$^{+/-}$ embryos, the severity was dramatically increased, resulting in loss of most of the anterior forebrain, which was designated a class IV defect (*n*=13; Table 2; Fig. 2G-I; supplementary material Fig. S1H,I). Wholemount in situ hybridisation against *Foxg1* and *Pax6* demonstrated the specific loss of anterior forebrain (*n*=3 per marker; Fig. 2H,I). Likewise, the expression domain of *Fgf8* at the ANR was absent, but normal *Fgf8* staining was observed at the mid-hindbrain boundary in all embryos analysed, confirming the loss of forebrain but not midbrain tissue (*n*=3; Fig. 2G,G′).

Together, these experiments suggest that a minimum gene dosage of *Hesx1* and *Tcf3* is required for normal development of the forebrain.

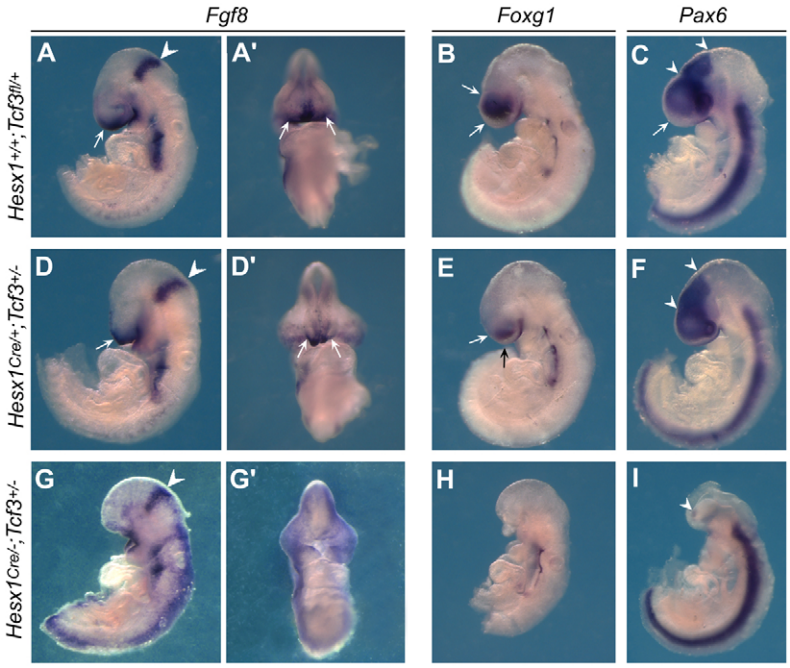

Fig. 2. Gene dosage-dependent forebrain defects in mouse embryos genetically deficient for *Hesx1* and *Tcf3*. In situ hybridisation with *Fgf8*, *Foxg1* and *Pax6* antisense riboprobes on 9.5 dpc embryos. (**A**,**A′**) *Fgf8* expression in the wild-type brain is restricted to the anterior neural ridge (ANR, arrows) and at the mid-hindbrain boundary (MHB, arrowhead). Lateral view in A, frontal in A′. (**B**) *Foxg1* is expressed in the normal developing telencephalic vesicles (arrows). (**C**) In the wild-type brain, *Pax6* is expressed in the dorsal telencephalon (arrow), posterior forebrain (arrowheads) and eye. (**D**,**D′**) In *Hesx1*$^{Cre/+}$;*Tcf3*$^{+/-}$ double heterozygotes, *Fgf8* expression in the MHB (arrowheads) is normal but is reduced in the ANR (arrows). (**E**) *Foxg1* expression in the telencephalon is severely reduced in *Hesx1*$^{Cre/+}$;*Tcf3*$^{+/-}$ embryos (arrows). (**F**) *Pax6* expression in the telencephalon and eye is decreased but expression in the posterior forebrain is normal (arrowheads). (**G-I**) Forebrain defects are very severe in *Hesx1*$^{Cre/-}$;*Tcf3*$^{+/-}$ embryos and most of the forebrain is missing, as evidenced by the lack of *Fgf8* (G,G′) and *Foxg1* (H) expression. Note the normal expression of *Fgf8* in the MHB (arrowhead in G) and the minimal expression of *Pax6* (arrowhead in I).

Table 3. Genotypes of embryos from *Hesx1*$^{Cre/+}$;*Tcf3*$^{+/-}$ × *Tcf3*$^{fl/fl}$ crosses, classified according to severity of anterior defects

		Class of forebrain defects				
Genotype	Number of embryos	None	I	II	III	IV
Hesx1$^{Cre/+}$;*Tcf3*$^{fl/-}$	60	12	9	13	15	11
Hesx1$^{Cre/+}$;*Tcf3*$^{fl/+}$	47	39	8	–	–	–
Hesx1$^{+/+}$;*Tcf3*$^{fl/+}$	59	57	2	–	–	–
Hesx1$^{+/+}$;*Tcf3*$^{fl/-}$	52	52	–	–	–	–
Total	218					

*See Table 2 for class definitions.

Tcf3 is required in anterior neural progenitors for normal forebrain development

In mouse embryos, *Hesx1* is initially expressed in the anterior visceral endoderm at the onset of gastrulation at 6.5 dpc, in the anterior mesendoderm by 7.5 dpc and subsequently in the anterior neural ectoderm from 7.5-8.0 dpc (Thomas and Beddington, 1996). *Tcf3* is expressed in the epiblast at pre-gastrulation stages and in the anterior mesendoderm and anterior neural plate at 7.5 dpc in a broader domain than *Hesx1* (Merrill et al., 2004). In zebrafish, *hesx1* and *tcf3a* show similar expression domains, comprising mainly the anterior neural plate with weak expression in the anterior mesendoderm (Dorsky et al., 2003; Kim et al., 2000; Spieler et al., 2004). Therefore, the genetic interaction between *Hesx1* and *Tcf3* might occur at the anterior mesendoderm and/or the anterior neural ectoderm, where both factors are expressed (Merrill et al., 2004).

We aimed to define more precisely the tissue in which this interaction is required by using two mouse strains: (1) a conditional *Tcf3* mouse line in which exon 2 is flanked by *loxP* sites, generating a frameshift and premature termination of the protein upon Cre-mediated excision (Nguyen et al., 2009); and (2) the *Hesx1-Cre* knock-in strain described previously (Andoniadou et al., 2007). First, we assessed the pattern of Cre activity in *Hesx1*$^{Cre/+}$;*R26*$^{YFP/+}$ embryos at the presomitic and early somite stages. Abundant Cre-mediated excision, revealed by YFP expression, was first observed in the neuroectoderm in the 1- to 2-somite embryo, but little or no YFP expression was detected in the anterior mesendoderm-derived tissues such as the anterior foregut (supplementary material Fig. S2A; *n*=5 *Hesx1*$^{Cre/+}$;*R26*$^{YFP/+}$ embryos). This indicates that the *Hesx1-Cre* mouse strain drives Cre expression predominantly in the rostral neuroectoderm fated to become the anterior forebrain (supplementary material Fig. S1B) (Andoniadou et al., 2007). Second, we analysed whether the expression of *Dkk1* and *Shh*, two axial mesendoderm markers required for normal brain formation, could be affected in *Hesx1*$^{Cre/+}$;*Tcf3*$^{fl/-}$ embryos. In situ hybridisation revealed no significant differences in mRNA expression of these two markers in *Hesx1*$^{Cre/+}$;*Tcf3*$^{fl/-}$ or *Hesx1*$^{Cre/+}$;*Tcf3*$^{+/-}$ embryos compared with controls (supplementary material Fig. S2B,C; data not shown). These data suggest that the axial mesendoderm is unlikely to be affected in *Hesx1*$^{Cre/+}$;*Tcf3*$^{fl/-}$ or *Hesx1*$^{Cre/+}$;*Tcf3*$^{+/-}$ embryos and, together with the Cre-mediated excision analysis, support the view that conditional excision of *Tcf3* through the *Hesx1-Cre* allele, as well as the gene interaction between these two transcription factors, are likely to occur solely in the anterior neuroectoderm.

Approximately 80% of *Hesx1*$^{Cre/+}$;*Tcf3*$^{fl/-}$ embryos showed partially penetrant anterior forebrain defects ranging from normal development to unilateral microphthalmia/anophthalmia and/or small telencephalic vesicles (Table 3, class I-III; Fig. 3H-J), but ~20% of mutants displayed forebrain truncations comparable to those observed in *Hesx1*$^{Cre/-}$;*Tcf3*$^{+/-}$ embryos (Table 3, class IV; Fig. 3E-G). Proliferation and apoptosis analyses revealed comparable levels between mutants and controls (supplementary material Fig. S3), as previously shown in *Hesx1*$^{-/-}$ embryos (Andoniadou et al., 2007). Molecular analyses using *Foxg1*, *Fgf8* and *Pax6* markers revealed a reduction in their expression domains correlating with defect severity, in keeping with the loss of forebrain tissue at 9.5 dpc (*n*=13; Fig. 3E-J). Despite this reduction, the zona limitans intrathalamica was detected by *Shh* expression and the dorsal thalamus and hypothalamus were patterned properly as assessed by *Gbx2* and *Nkx2-1* expression, respectively (supplementary material Fig. S4).

Since, in zebrafish, *tcf3*-mediated repression of Wnt/β-catenin targets is required for normal brain development (Dorsky et al., 2003; Kim et al., 2000), we reasoned that if a derepression of Wnt targets is taking place due to the loss of *Tcf3* in the anterior forebrain, hence activating the pathway, this should be evidenced by anteriorisation of targets activated by Wnt expression. The direct Wnt/β-catenin/TCF/LEF target *Sp5* (Weidinger et al., 2005) is normally expressed in the midbrain but is absent from the anterior forebrain (Fig. 3C). By contrast, the *Sp5* expression domain was rostrally expanded in the anterior forebrain of *Hesx1*$^{Cre/+}$;*Tcf3*$^{fl/-}$ embryos (*n*=4; Fig. 3D). Expression of *Six3*, an essential repressor during normal forebrain development, is negatively regulated by the Wnt signalling pathway (Braun et al., 2003; Lagutin et al., 2003). In agreement with this notion and the ectopic expression of *Sp5* in the anterior forebrain, the *Six3* expression domain in the anterior neural plate was markedly reduced in *Hesx1*$^{Cre/+}$;*Tcf3*$^{fl/-}$ embryos at the 5- to 8-somite stage (Fig. 3B,B′). Often, *Six3* expression was asymmetric in *Hesx1*$^{Cre/+}$;*Tcf3*$^{fl/-}$ embryos (Fig. 3B). It is important to note that in the anterior forebrain of *Hesx1*$^{-/-}$ mutants, *Sp5* is ectopically expressed, whereas the *Six3* expression domain is reduced and asymmetric defects are also observed (Andoniadou et al., 2007; Dattani et al., 1998).

In summary, three main conclusions can be drawn from these results: (1) in mouse, *Tcf3* is required in anterior forebrain precursors, where it prevents the ectopic expression of Wnt/β-catenin targets; (2) there is a genetic interaction between *Hesx1* and *Tcf3* in the anterior neuroectoderm; and (3) the similar molecular and morphological defects observed in *Hesx1*$^{Cre/-}$, *Hesx1*$^{Cre/+}$;*Tcf3*$^{fl/-}$ and *Hesx1*$^{Cre/+}$;*Tcf3*$^{+/-}$ embryos suggest that both factors synergise in a gene dosage-dependent manner to maintain the anterior character of anterior forebrain progenitors.

Conditional removal of β-catenin partially rescues the anterior forebrain defects of *Hesx1* null mutants

The genetic analyses described above on *Hesx1*-deficient and *Hesx1/Tcf3* compound embryos suggest that the posteriorisation of anterior forebrain precursors leading to anterior truncations is driven by the derepression of Wnt/β-catenin targets and the ectopic activation of the pathway in the anterior neural plate. To test this

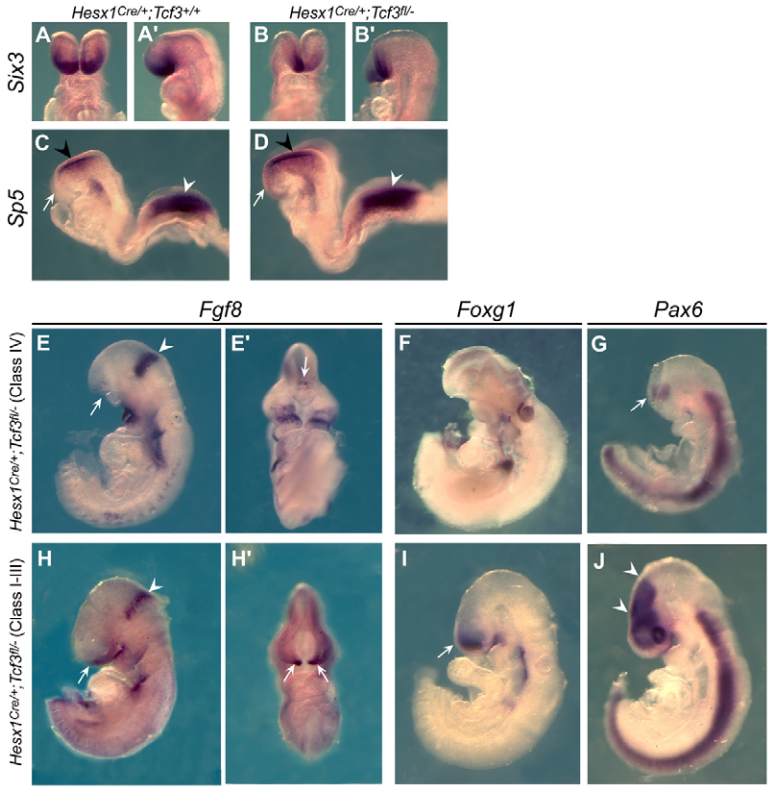

Fig. 3. *Tcf3* is required within the anterior neuroectoderm for normal mouse forebrain development. (**A-D**) In situ hybridisation with *Six3* and *Sp5* antisense riboprobes on 8.5 dpc *Hesx1*$^{Cre/+}$;*Tcf3*$^{fl/-}$ (B,B′) and control *Hesx1*$^{Cre/+}$;*Tcf3*$^{+/+}$ (A,A′) embryos. Expression of *Six3*, a marker of the anterior forebrain primordium in 8.5 dpc embryos, is reduced in the *Hesx1*$^{Cre/+}$;*Tcf3*$^{fl/-}$ mutant compared with the control. By contrast, the expression domain of *Sp5*, a direct Wnt/β-catenin target gene, is rostrally expanded into the prospective forebrain region of the *Hesx1*$^{Cre/+}$;*Tcf3*$^{fl/-}$ mutant (arrow in D) as compared with a control embryo, which does not express *Sp5* in the prospective forebrain (arrow in C). The arrowheads in C and D denote *Sp5* expression in the midbrain (black) and tailbud (white). (**E-J**) In situ hybridisation with *Fgf8*, *Foxg1* and *Pax6* antisense riboprobes on 9.5 dpc *Hesx1*$^{Cre/+}$;*Tcf3*$^{fl/-}$ embryos with severe (class IV) or mild (class I-III) forebrain defects. Stage-matched wild-type controls are shown in Fig. 2A-C. (E,E′) *Fgf8* expression at the ANR is severely reduced (arrow in E), with only a minimal domain of expression remaining (arrow in E′); however, expression at the MHB remains normal (arrowhead in E). In an embryo with severe anterior truncation (F), *Foxg1* expression, which is normally at the telencephalic vesicles, is lost. Similarly, the anterior *Pax6* expression domain is almost absent due to the loss of forebrain tissue and only a small patch of *Pax6*-positive cells, probably corresponding to posterior forebrain, is detectable (arrow in G). In mildly affected *Hesx1*$^{Cre/+}$;*Tcf3*$^{fl/-}$ mutants, the *Fgf8* expression domain at the ANR is reduced and restricted to the midline (arrows in H,H′), but MHB expression is unaffected (arrowhead in H). *Foxg1* expression in the telencephalon is severely reduced in a mildly affected *Hesx1*$^{Cre/+}$;*Tcf3*$^{fl/-}$ embryo (arrow in I). In these embryos, *Pax6* expression in the telencephalon and eye is decreased but expression in the posterior forebrain is normal (arrowheads in J).

hypothesis further, we used the *BATgal* transgenic mouse line, which provides a *lacZ* reporter for active β-catenin/TCF/LEF signalling (Maretto et al., 2003). X-Gal staining of *Hesx1*$^{Cre/+}$;*BATgal* and *BATgal* embryos revealed no significant differences in the β-galactosidase staining pattern and the anterior forebrain remained unstained, demonstrating the low or absent signalling mediated by β-catenin/TCF/LEF in the anterior region of the neural plate (Fig. 4A,A′; data not shown). By contrast, *Hesx1*$^{Cre/-}$;*BATgal* mutant embryos displayed a clear anteriorisation of X-Gal staining into the rostral neural plate, relative to controls (Fig. 4B,B′). This ectopic β-galactosidase expression in the absence of *Hesx1* strongly suggests that there is an activation of Wnt/β-catenin signalling in the anterior forebrain of these mutants.

We reasoned that downregulation of this signalling pathway would result in the improvement of the defective patterning and development of the anterior neural plate in *Hesx1*-deficient mutants. We used a genetic approach to reduce the levels of β-catenin (*Ctnnb1*) expression, and therefore ameliorate the levels of Wnt/β-catenin signalling in *Hesx1*-deficient mutants. Previously described *Hesx1*$^{+/-}$ and *Ctnnb1*$^{+/-}$ strains, each carrying a null allele, are both viable and fertile (Dattani et al., 1998; Haegel et al., 1995). We generated *Hesx1*$^{+/-}$;*Ctnnb1*$^{+/-}$ compound mice, which were also normal and fertile. By crossing these animals to *Hesx1*$^{+/-}$ mice we generated *Hesx1*$^{-/-}$;*Ctnnb1*$^{+/-}$ and control *Hesx1*$^{-/-}$;*Ctnnb1*$^{+/+}$ embryos. Morphological comparisons did not reveal significant differences in the severity of anterior forebrain defects between these two genotypes (supplementary material Table S1; *n*=181 embryos), and haploinsufficiency of *Ctnnb1* did not restore forebrain development in the *Hesx1*$^{-/-}$;*Ctnnb1*$^{+/-}$ mutants relative to *Hesx1*$^{-/-}$;*Ctnnb1*$^{+/+}$ controls.

To remove both copies of β-catenin, we used a conditional approach resulting in the specific deletion of *Ctnnb1* only in *Hesx1*-expressing cells. By crossing the *Hesx1-Cre* driver with a *Ctnnb1* loss-of-function strain in which exons 2-6 are flanked by *loxP* sites [*Ctnnb1-lox(ex2-6)*, hereafter *Ctnnb1-LOF*] (Brault et al., 2001), we overcame the gastrulation defect of *Ctnnb1*$^{-/-}$ embryos (Haegel et al., 1995). We generated embryos completely lacking *Hesx1* and conditionally null for *Ctnnb1* in the forebrain (*Hesx1*$^{Cre/-}$;*Ctnnb1*$^{LOF/-}$) through crossing *Hesx1*$^{Cre/+}$;*Ctnnb1*$^{+/-}$ with *Hesx1*$^{+/-}$;*Ctnnb1*$^{LOF/+}$ animals (supplementary material Fig.

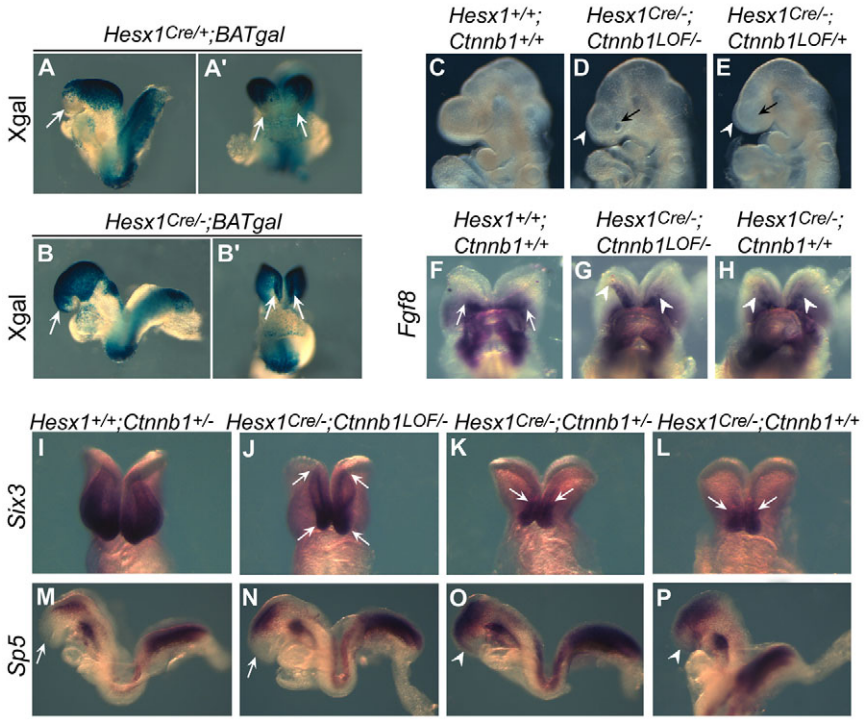

Fig. 4. Loss of function of β-catenin is sufficient to improve forebrain patterning in mouse *Hesx1$^{Cre/-}$;Ctnnb1$^{LOF/-}$* embryos. (**A**,**A′**) X-Gal staining reveals *BATgal* activity in the neural plate of *Hesx1$^{Cre/+}$;BATgal* control embryo at 8.5 dpc, but the anteriormost forebrain is not stained (arrows). (**B**,**B′**) By contrast, in the *Hesx1$^{Cre/-}$* mutant, the anterior forebrain is *BATgal* positive, suggesting ectopic activation of the Wnt/β-catenin signalling pathway (arrows). (**C-E**) The conditional inactivation of β-catenin in a *Hesx1$^{Cre/-}$;Ctnnb1$^{LOF/-}$* embryo (D) leads to a significant improvement of telencephalic (arrowhead) and eye (arrow indicating the presence of an optic vesicle) development compared with a *Hesx1$^{Cre/-}$;Ctnnb1$^{LOF/+}$* embryo (E). However, compared with a wild-type control embryo (C), this is not a full restoration to normal development. (**F-H**) Frontal views of embryos after in situ hybridisation with antisense riboprobes against *Fgf8*. Normal expression at the ANR of a wild-type embryo at 3-5 somites (arrows in F). In *Hesx1$^{Cre/-}$* mutants, the expression of *Fgf8* at the ANR is reduced and restricted to the midline (arrowheads in H). In the *Hesx1$^{Cre/-}$;Ctnnb1$^{LOF/-}$* embryo (G) there is an asymmetric expansion in *Fgf8* expression compared with the homozygous *Hesx1* mutant (H). Arrowheads indicate the limit of *Fgf8* expression, with broader expression on the right-hand side. An asymmetric improvement of forebrain defects in *Hesx1$^{Cre/-}$;Ctnnb1$^{LOF/-}$* embryos is often seen at later stages. (**I-P**) In situ hybridisation with antisense riboprobes against *Six3* and *Sp5* on 8.5 dpc embryos at 8-10 somites. The *Six3* expression domain in the anterior forebrain of the *Hesx1$^{Cre/-}$;Ctnnb1$^{LOF/-}$* embryo (arrows in J) is larger than in *Hesx1$^{Cre/-}$;Ctnnb1$^{+/-}$* and *Hesx1$^{Cre/-}$* mutants (arrows in K,L), but smaller than in the control embryo (I). Expression of the Wnt/β-catenin direct target gene *Sp5* is normally excluded from the anterior forebrain (arrow in M), and it remains so in the *Hesx1$^{Cre/-}$;Ctnnb1$^{LOF/-}$* embryo (arrow in N). However, ectopic *Sp5* expression is detected in the anterior forebrain of *Hesx1$^{Cre/-}$;Ctnnb1$^{+/-}$* and *Hesx1$^{Cre/-}$* mutants (arrowheads in O,P).

S5). Analysis of *Hesx1$^{Cre/-}$;Ctnnb1$^{LOF/-}$* embryos between 9.5 dpc and 15.5 dpc demonstrated a shift in the range of forebrain defects to a milder spectrum (ranging from normal to class II, Table 4; n=12) than those observed in *Hesx1$^{Cre/-}$;Ctnnb1$^{LOF/+}$*, *Hesx1$^{Cre/-}$;Ctnnb1$^{+/+}$* or *Hesx1$^{Cre/-}$;Ctnnb1$^{+/-}$* littermates (classes II-III, n=45) (Table 4; supplementary material Table S2; Fig. 4D; P<0.001, two-tailed Fisher's exact test).

This phenotypic rescue of forebrain development was also supported by an overall improvement of anterior neural plate patterning in *Hesx1$^{Cre/-}$;Ctnnb1$^{LOF/-}$* embryos. The *Fgf8* expression domain in the ANR of *Hesx1$^{Cre/-}$* mutants is small and appears restricted to the medial region of the neural plate (Fig. 4H; n=3). In *Hesx1$^{Cre/-}$;Ctnnb1$^{LOF/-}$* 'rescued' mutants, we observed a lateral expansion of the *Fgf8* expression domain (Fig. 4G); in some cases, this improvement was asymmetric, consistent with a frequent asymmetric improvement of forebrain tissue at later stages. Related to this, expression of the anterior forebrain marker *Six3* occurred over a broader domain of anterior neural plate in rescued embryos as compared with *Hesx1* null mutants, as more forebrain tissue was correctly specified at 8.5 dpc (Fig. 4J; n=4). Whereas in *Hesx1* null mutants, expression of the Wnt target *Sp5* was rostrally expanded, reaching the anterior tip of the neural plate even prior to any evidence of a reduction in tissue (Andoniadou et al., 2007) (Fig. 4O,P; n=6), in *Hesx1$^{Cre/-}$;Ctnnb1$^{LOF/-}$* mutants at 8.5 dpc, no *Sp5* transcripts were detected in the anterior forebrain, confirming a restoration of normal patterning (Fig. 4N; n=3).

Together, these results demonstrate that ectopic anterior activation of the Wnt/β-catenin signalling pathway plays an essential role in the pathogenesis of the forebrain defects in *Hesx1*-deficient mutants.

Absence of *Hesx1* leads to the ectopic activation of multiple Wnt/β-catenin target genes in anterior forebrain progenitors

Our results demonstrate that conditional removal of *Ctnnb1* in the anterior forebrain leading to a reduction of Wnt/β-catenin signalling is sufficient to improve forebrain patterning in *Hesx1$^{Cre/-}$* mutants, strongly suggesting that the mechanisms underlying the forebrain defects in *Hesx1*-deficient embryos are mediated by the ectopic activation of Wnt/β-catenin signalling in the anterior neural plate. We investigated this hypothesis further by performing gene profiling analyses, comparing anterior forebrain precursors expressing and not

Table 4. Genotypes of embryos from *Hesx1*$^{Cre/+}$;*Ctnnb1*$^{+/-}$ × *Hesx1*$^{+/-}$;*Ctnnb1*$^{LOF/+}$ crosses, classified according to severity of anterior defects

		Class of forebrain defects				
Genotype*	Number of embryos	None	I	II	III	IV
Hesx1$^{Cre/-}$;*Ctnnb1*$^{LOF/-}$	12	2	5	5	–	–
Hesx1$^{Cre/-}$;*Ctnnb1*$^{LOF/+}$	20	–	–	9	11	–
Hesx1$^{Cre/-}$;*Ctnnb1*$^{+/+}$	13	–	–	7	6	–
Hesx1$^{Cre/-}$;*Ctnnb1*$^{+/-}$	12	–	–	5	7	–
Hesx1$^{Cre/+}$;*Ctnnb1*$^{LOF/-}$	9	9	–	–	–	–
Hesx1$^{Cre/+}$;*Ctnnb1*$^{LOF/+}$	15	15	–	–	–	–
Hesx1$^{Cre/+}$;*Ctnnb1*$^{+/+}$	9	9	–	–	–	–
Hesx1$^{Cre/+}$;*Ctnnb1*$^{+/-}$	9	9	–	–	–	–
Total	198					

*Only relevant genotypes are shown. For a full list of genotypes, see supplementary material Table S2.
‡See Table 2 for class definitions.

expressing *Hesx1* at the 3- to 5-somite stage, just when the first morphological and molecular abnormalities are detectable in *Hesx1*-deficient mutants. Because the *Hesx1* expression domain is very restricted at this stage, we generated a *Hesx1-eGFP* knock-in mouse line by replacing the *Hesx1* coding region with *eGFP* as a tool to flow sort this small population of forebrain progenitors (Fig. 5A). This enabled us to avoid the contamination from *Hesx1* non-expressing cells that would be present if performing this analysis using whole embryos or micro-dissected regions.

Hesx1$^{eGFP/+}$ mice were normal and fertile and embryos showed fluorescence in the anterior neural plate (Fig. 5C) in a pattern identical to endogenous *Hesx1* expression. By contrast, *Hesx1*$^{eGFP/eGFP}$ embryos (Fig. 5D) showed the anterior forebrain defects observed in *Hesx1*-deficient embryos and the pattern of fluorescence was faithful to the residual anterior forebrain domain in these mutants, which is restricted to the most anteromedial region of the neural plate and is marked by *Six3* expression (Martinez-Barbera et al., 2000).

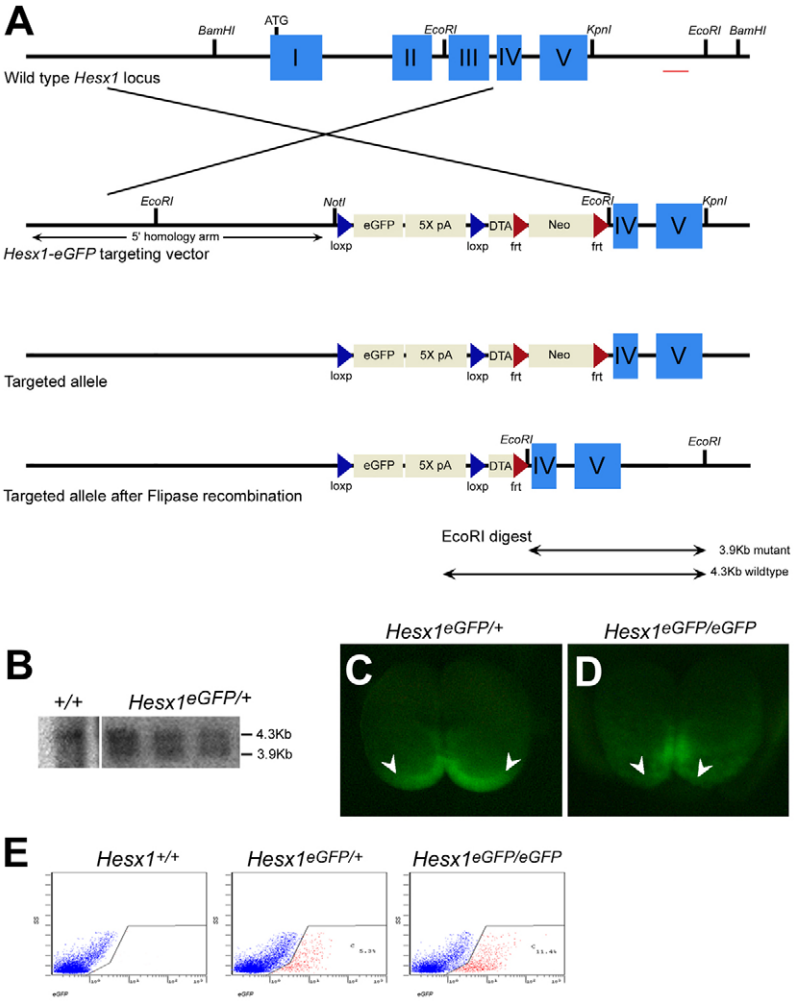

Fig. 5. Purification of anterior forebrain precursors by flow sorting from *Hesx1*$^{eGFP/+}$ and *Hesx1*$^{eGFP/eGFP}$ mouse embryos. (**A**) Targeting strategy for the generation of the *Hesx1-eGFP* allele. Top to bottom: structure of the murine *Hesx1* locus; *Hesx1-eGFP* targeting vector; targeted allele prior to and after flipase-mediated excision of the *Neo* cassette; expected bands for the targeted and wild-type alleles after Southern blot analysis of DNA samples digested with *Eco*RI and hybridised with an external probe (red line in top schematic). The DTA cassette is irrelevant to this study as it has not been activated in the presence of Cre in the experiments presented here. (**B**) Southern blot analysis of wild-type (*Hesx1*$^{+/+}$) and *Hesx1*$^{eGFP/+}$ ES cell clones digested with *Eco*RI and hybridised with an external probe (red line in A). Only the 4.3 kb wild-type band is detected in the *Hesx1*$^{+/+}$ sample, whereas both wild-type and mutant (3.9 kb) bands are detected in three correctly targeted *Hesx1*$^{eGFP/+}$ clones. (**C**) Dorsal view of the neural plate of a 3-somite stage *Hesx1*$^{eGFP/+}$ embryo showing eGFP fluorescence in the anterior forebrain primordium during normal development (arrowheads). (**D**) In the *Hesx1*$^{eGFP/eGFP}$ embryo, in which there is no *Hesx1* expression, the anterior forebrain domain marked by eGFP fluorescence becomes medially restricted (arrowheads). (**E**) Flow sorting of dissociated whole embryos between 3 and 5 somites allows the specific isolation of cells from the prospective anterior forebrain through eGFP fluorescence from the *Hesx1* locus. Scatter plots from a representative experiment are shown. Purified cells from heterozygous *Hesx1*$^{eGFP/+}$ (normal) or homozygous *Hesx1*$^{eGFP/eGFP}$ mutant embryos were used for RNA isolation and subsequent microarray analysis.

Microarray analysis of anterior forebrain precursors isolated by flow sorting from *Hesx1*$^{eGFP/+}$ and *Hesx1*$^{eGFP/eGFP}$ 3- to 5-somite embryos (Fig. 5) confirmed changes in gene expression that we had previously characterised by wholemount in situ hybridisation on *Hesx1* null mutants (Andoniadou et al., 2007). For example, by wholemount in situ hybridisation, *Foxg1* and *Pax6* expression domains were reduced in the *Hesx1*$^{Cre/–}$ mutant anterior forebrain compared with *Hesx1*$^{Cre/+}$ or *Hesx1*$^{+/+}$ controls. In the microarray (full data can be found at ArrayExpress with ID: E-MEXP-2586), levels of *Foxg1* and *Pax6* expression were found to be 1.86-fold and 1.81-fold higher, respectively, in the *Hesx1*$^{eGFP/+}$ heterozygous relative to the *Hesx1*$^{eGFP/eGFP}$ homozygous anterior forebrain precursors. Conversely, the expression domains of *Wnt1*, *Wnt3a*, *Foxd3* and *Pax3* were increased in the *Hesx1* null mutant anterior forebrain when visualised by wholemount in situ hybridisation (Andoniadou et al., 2007), and this is recapitulated in the microarray as they showed a 1.6-, 3.2-, 1.61- and 1.69-fold increase in the *Hesx1*$^{eGFP/eGFP}$ anterior forebrain cells, respectively. Finally, *Hesx1* itself, as expected, showed substantially higher (9.2-fold) expression in the *Hesx1*$^{eGFP/+}$ heterozygous anterior forebrain precursors, ranking as the highest statistically significant differentially expressed gene in the heterozygous sample, corroborating the purity of the mutant cell population and the robustness of the microarray data.

Following an unbiased approach, stringent statistical measures and multiple testing correction, we revealed 55 genes that were expressed at significantly higher levels in the *Hesx1*$^{eGFP/eGFP}$ homozygous null mutant anterior forebrain progenitors and 18 genes that were expressed at significantly lower levels (Table 5). This is line with previous research suggesting that HESX1 normally functions as a transcriptional repressor (Carvalho et al., 2010; Dasen et al., 2001; Ermakova et al., 1999; Ermakova et al., 2007). Validation by qRT-PCR on independent samples was carried out for a selection of genes from this shortlist and all 19 genes queried displayed the same trend observed in the microarray (supplementary material Fig. S6). Among the upregulated genes, a significant proportion (20%) were associated with the Wnt pathway, including *Tnfrsf19*, *Dixdc1*, *Sp5*, *Apcdd1* and *Tnik*. A further 46% were associated with processes positively regulated by enhancement of Wnt signalling, namely neural crest specification (16%; e.g. *Sox10*, *Twist1*, *Ednra*, *Ednrb*) and neural differentiation (30%; *Neurog1*, *Ngfr*, *Mef2c*, *Nr2f1*, *Nrp2*).

Certain genes that are known to be upregulated in the forebrain of the *Hesx1*-deficient embryos, as judged by in situ hybridisation, e.g. the Wnt target *Axin2* (Andoniadou et al., 2007), did not pass the strict criteria that we set for statistically significant differences so we also analysed all genes by their Gene Ontology annotations and grouped them by involvement in specific pathways, with differences of 1.6-fold as cut-off. Key components, main effectors and downstream target genes of the major morphogenetic pathways dependent on SHH, FGF or BMP/TGFβ were largely unaffected (supplementary material Tables S3-S5). By contrast, multiple components of the canonical Wnt signalling pathway were upregulated in *Hesx1*$^{eGFP/eGFP}$ cells. When subdivided into receptors, ligands, intracellular components, negative regulators and target genes, it became clear that a large number of Wnt targets were expressed at higher levels in the absence of the repressor HESX1 (15 out of 37 genes queried, over 1.6-fold upregulated; supplementary material Table S6). The levels of Wnt receptors and

Table 5. Genes expressed at significantly different levels in pairwise microarray comparison of *Hesx1*$^{eGFP/+}$ and *Hesx1*$^{eGFP/eGFP}$ anterior forebrain cells

		Higher expression in *Hesx1*$^{eGFP/eGFP}$		Higher expression in *Hesx1*$^{eGFP/+}$	
Gene	Fold change	Gene	Fold change	Gene	Fold change
Dlx2	6.158	*Ets1*	2.751	*Pnma2*	–1.803
Laptm5	5.556	*Cerkl*	2.747	*A330094K24Rik*	–1.82
Lect1	5.276	***Enpp2***	2.712	*Gm4988*	–1.824
Npr3	5.208	*Emilin1*	2.705	*Zfp185*	–1.877
B930025B16Rik	5.025	*Mcc*	2.703	*Lrrn1*	–1.913
Neurog1	4.53	*Guca1a*	2.681	***Shisa2***	–1.916
Ngfr	4.337	*Nr2f1*	2.667	*Pcsk2*	–2.103
Anxa1	4.253	*Fam81a*	2.656	*Glrx*	–2.11
Mef2c	4.121	*Gm12688*	2.597	*Ermn*	–2.251
Tnik	3.759	*Bach2*	2.547	*BC016495*	–2.414
Tmem119	3.749	*Rbms3*	2.526	*Fezf1*	–2.49
Sim2	3.679	***Twist1***	2.487	*Bdp1*	–2.534
Ednrb	3.548	*Phactr1*	2.46	*Efhd1*	–2.681
Itga8	3.524	*Col5a2*	2.43	*Ptger4*	–3.004
Erbb3	3.507	*Gfra2*	2.288	*Eno4*	–3.124
Ednra	3.4	*Sdc3*	2.279	*4930506M07Rik*	–3.182
Hapln1	3.326	***Wnt6***	2.265	*Lhx2*	–3.499
L1cam	3.25	*Igsf3*	2.242	*Hesx1*	–9.156
Wnt3a	3.205	*Pdgfra*	2.142		
Elk3	3.166	*Sphk1*	2.139		
Elfn1	3.064	***Dixdc1***	2.136		
4930452G13Rik	2.933	***Sp5***	2.121		
Tnfrsf19	2.932	*Tmc6*	2.094		
Dlc1	2.932	*Gfra1*	2.092		
Plp1	2.858	*Sox10*	1.951		
Rasa3	2.857	*Rhbdf1*	1.864		
Col9a1	2.842	***Apcdd1***	1.852		
Nrp2	2.809				

Positive value denotes higher expression in *Hesx1*$^{eGFP/eGFP}$ and negative value denotes higher expression in *Hesx1*$^{eGFP/+}$. Known targets, components and regulators of the Wnt pathway are in bold.

Wnt ligands remained unchanged, except for an increase in the expression of *Wnt1*, *Wnt3a* and *Wnt6* (Table 5; supplementary material Table S7). Notably, expression of *Ctnnb1* was unaffected in $Hesx1^{eGFP/eGFP}$ cells, as was the expression of genes encoding components of the destruction complex, such as *Axin1*, *Gsk3b*, *Csk1a1* and *Apc*, demonstrating that the pathway was not affected at the level of regulation of *Ctnnb1* expression or of components affecting degradation of β-catenin protein (supplementary material Table S8).

Together, this gene expression analysis demonstrates that the absence of HESX1 leads to the ectopic activation of numerous Wnt target genes in anterior forebrain progenitors.

DISCUSSION

In this study, we provide novel genetic and molecular data demonstrating that the homeobox gene *Hesx1* antagonises the activation of Wnt/β-catenin signalling in early forebrain progenitors in zebrafish and mouse embryos. In addition, using genetic approaches we reveal a previously unidentified requirement for *Tcf3* in these progenitors, where it interacts with *Hesx1* to promote anterior character.

Novel function of *hesx1* in zebrafish forebrain development

Hesx1 has previously been shown to play an essential role during normal forebrain and pituitary development in *Xenopus*, mice and humans. Here, we show that *hesx1* zebrafish morphants display forebrain defects in the sensitised *hdl* background that are reminiscent of those observed in *Hesx1*-deficient mouse embryos. These defects are rescued by injection of murine *Hesx1* mRNA, suggesting a functional conservation in both species. Significant amino acid sequence homology between Hesx1 proteins of zebrafish and mouse is restricted to the homeobox (DNA-binding domain) at the C-terminus and the engrailed homology 1 (eh1) domain at the N-terminus, which interacts with Groucho/TLE members to mediate transcriptional repression (Carvalho et al., 2010; Dasen et al., 2001). This suggests that the main molecular function of Hesx1/Anf family members is to act as transcriptional repressors.

Members of the TCF/LEF family, including TCF3, activate transcription of Wnt target genes upon association with β-catenin. They are also able to repress genes through association with Groucho/TLE1 co-repressors, an interaction that displaces their association with β-catenin. In the zebrafish embryo, loss of Tcf3a repressor activity was shown to be solely responsible for the anterior truncations displayed in the *hdl* mutants. Injection of mRNA encoding a truncated form of Tcf3a that lacks the N-terminal β-catenin-interacting domain was capable of rescuing the mutant phenotype through its repressor function. Furthermore, overexpression of the DNA-binding domain fused to the engrailed repressor domain was also able to rescue the *hdl* anterior defects; however, when fused to the VP16 activator domain it not only failed to rescue this phenotype but also induced forebrain truncations in wild-type embryos (Kim et al., 2000).

Together, these experiments and our MO injections on a sensitised *hdl* background suggest that there is a functional interaction between Hesx1 and Tcf3a factors that prevents the expression of Wnt targets in the zebrafish embryo. Therefore, the lack of a phenotype in the *hesx1* zebrafish morphant could be a consequence of genetic redundancy, whereby Tcf3 factors compensate for the lack of Hesx1.

Tcf3 and *Hesx1* genetically interact in the zebrafish and mouse embryo to antagonise Wnt/β-catenin signalling activation in anterior forebrain progenitors

In the zebrafish embryo, Tcf3 acts independently of β-catenin for normal forebrain development by maintaining the repression of Wnt/β-catenin target genes. Our data extend this analysis and provide evidence that *Tcf3* plays this role specifically within the forebrain neuroectoderm. Compound embryos carrying a distinct gene dosage of *Hesx1* and *Tcf3* show telencephalic and eye defects that are similar to those observed in single-mutant embryos deficient for either *Hesx1* or *Tcf3*. This genetic interaction suggests a requirement not only for TCF3 but also for HESX1 in the inhibition of Wnt/β-catenin target expression in anterior forebrain precursors. We cannot rule out a weak interaction in the axial mesendoderm, but our *Dkk1* and *Shh* analyses suggest that this tissue is unlikely to be affected.

Confirming a novel function of HESX1 in antagonising Wnt signalling, we show that the $Hesx1^{-/-}$ forebrain defects are partially rescued and forebrain patterning improved in $Hesx1^{Cre/-};Ctnnb1^{LOF/-}$ embryos, in which aberrant Wnt signalling is prevented specifically in anterior forebrain precursors. This illustrates that the forebrain abnormalities in *Hesx1*-deficient mutants are indeed caused by an ectopic response to this pathway. Deletion of *Ctnnb1* in *Foxg1-Cre;*$Ctnnb1^{LOF/-}$ embryos has previously been shown to cause forebrain defects (Junghans et al., 2005; Wang et al., 2010), which result from an increase in apoptosis following disruption of structural integrity due to the absence of β-catenin in the adherence junctions of neuroepithelial cells (Junghans et al., 2005) as well as the loss of *Fgf8* expression at the ANR (Paek et al., 2011; Wang et al., 2010). By contrast, we did not observe any forebrain phenotype in $Hesx1^{Cre/+};Ctnnb1^{LOF/-}$ embryos. This is possibly due to the different expression patterns of *Foxg1* and *Hesx1*, or is a potential additive effect due to *Foxg1* haploinsufficiency in the *Foxg1-Cre* knock-in line used, as even heterozygous animals have telencephalic defects (Eagleson et al., 2007).

Analysis of double-heterozygous embryos for *Hesx1* and another Wnt antagonist, *Six3*, have also revealed forebrain defects comparable to those of *Hesx1;Tcf3* compound mutant embryos (supplementary material Fig. S7) (Gaston-Massuet et al., 2008). Similar to the demonstration that *Hesx1* can antagonise Wnt signalling in the zebrafish forebrain, mouse *Six3* mRNA is able to rescue the *hdl* phenotype through antagonising Wnt signalling (Lagutin et al., 2003).

Finally, gene profiling analysis revealed a significant enhancement in the expression of genes relevant to Wnt signalling in the *Hesx1*-deficient anterior forebrain precursors relative to $Hesx1^{eGFP/+}$ heterozygous controls. The increase in expression of several target genes of the Wnt/β-catenin pathway in the $Hesx1^{eGFP/eGFP}$ anterior forebrain cells demonstrates the ectopic activation of this pathway in the absence of *Hesx1* in a tissue that would normally be unresponsive to Wnt signals. Indeed, in the $Hesx1^{eGFP/eGFP}$ population, we observe an increase in the Wnt effectors *Lef1* (1.7-fold) and *Tcf1* (*Tcf7*, 1.6-fold), which are not normally expressed in the anterior forebrain. The ectopic expression of *Sp5* in the forebrain of $Hesx1^{Cre/+};Tcf3^{fl/-}$ embryos leads to the notion of a similar underlying defect in these mutants. This supports the notion that *Hesx1* may act, in concert with *Tcf3* and *Six3*, as a negative regulator of the Wnt pathway in the anterior forebrain, furthering our understanding of the mechanisms required to establish forebrain identity. In addition, the microarray data

provide a valuable resource because they define the normal molecular signature of early anterior forebrain precursors. This information can be used for comparative studies with other mouse mutants or to assess the efficiency of protocols for in vitro differentiation of stem cell lines into neurons.

The variability in the forebrain defects observed in compound mutants also exists in human patients with mutations in *HESX1*. To date, more than 15 mutations have been identified in human *HESX1* in association with variable degrees of forebrain and pituitary defects (Kelberman et al., 2009). Our mouse research opens the possibility for mutations in genes with synergistic action, such as *TCF3*, to be candidates for modifying these phenotypes.

Acknowledgements
We thank Professor Andrew Copp for critical reading of the manuscript. This work was carried out with the support of the UCL Institute of Child Health and Great Ormond Street Hospital Flow Cytometry Core Facility, UCL Genomics, the ICH Embryonic Stem Cell/Chimera Production Facility and UCL Biological Services Unit.

Funding
This work was funded by the Wellcome Trust [grants 084361, 078432, 086545]. Deposited in PMC for release after 6 months.

Competing interests statement
The authors declare no competing financial interests.

Supplementary material
Supplementary material available online at
http://dev.biologists.org/lookup/suppl/doi:10.1242/dev.066597/-/DC1

References

Andoniadou, C. L., Signore, M., Sajedi, E., Gaston-Massuet, C., Kelberman, D., Burns, A. J., Itasaki, N., Dattani, M. and Martinez-Barbera, J. P. (2007). Lack of the murine homeobox gene Hesx1 leads to a posterior transformation of the anterior forebrain. *Development* **134**, 1499-1508.

Brannon, M., Brown, J. D., Bates, R., Kimelman, D. and Moon, R. T. (1999). XCtBP is a XTcf-3 co-repressor with roles throughout Xenopus development. *Development* **126**, 3159-3170.

Brantjes, H., Roose, J., van de Wetering, M. and Clevers, H. (2001). All Tcf HMG box transcription factors interact with Groucho-related co-repressors. *Nucleic Acids Res.* **29**, 1410-1419.

Brault, V., Moore, R., Kutsch, S., Ishibashi, M., Rowitch, D. H., McMahon, A. P., Sommer, L., Boussadia, O. and Kemler, R. (2001). Inactivation of the beta-catenin gene by Wnt1-Cre-mediated deletion results in dramatic brain malformation and failure of craniofacial development. *Development* **128**, 1253-1264.

Braun, M. M., Etheridge, A., Bernard, A., Robertson, C. P. and Roelink, H. (2003). Wnt signaling is required at distinct stages of development for the induction of the posterior forebrain. *Development* **130**, 5579-5587.

Buchert, M., Athineos, D., Abud, H. E., Burke, Z. D., Faux, M. C., Samuel, M. S., Jarnicki, A. G., Winbanks, C. E., Newton, I. P., Meniel, V. S. et al. (2010). Genetic dissection of differential signaling threshold requirements for the Wnt/beta-catenin pathway in vivo. *PLoS Genet.* **6**, e1000816.

Carvalho, L. R., Brinkmeier, M. L., Castinetti, F., Ellsworth, B. S. and Camper, S. A. (2010). Corepressors TLE1 and TLE3 interact with HESX1 and PROP1. *Mol. Endocrinol.* **24**, 754-765.

Dasen, J. S., Barbera, J. P., Herman, T. S., Connell, S. O., Olson, L., Ju, B., Tollkuhn, J., Baek, S. H., Rose, D. W. and Rosenfeld, M. G. (2001). Temporal regulation of a paired-like homeodomain repressor/TLE corepressor complex and a related activator is required for pituitary organogenesis. *Genes Dev.* **15**, 3193-3207.

Dattani, M. T., Martinez-Barbera, J. P., Thomas, P. Q., Brickman, J. M., Gupta, R., Martensson, I. L., Toresson, H., Fox, M., Wales, J. K., Hindmarsh, P. C. et al. (1998). Mutations in the homeobox gene HESX1/Hesx1 associated with septo-optic dysplasia in human and mouse. *Nat. Genet.* **19**, 125-133.

Dorsky, R. I., Itoh, M., Moon, R. T. and Chitnis, A. (2003). Two tcf3 genes cooperate to pattern the zebrafish brain. *Development* **130**, 1937-1947.

Eagleson, K. L., Schlueter McFadyen-Ketchum, L. J., Ahrens, E. T., Mills, P. H., Does, M. D., Nickols, J. and Levitt, P. (2007). Disruption of Foxg1 expression by knock-in of cre recombinase: effects on the development of the mouse telencephalon. *Neuroscience* **148**, 385-399.

Ermakova, G. V., Alexandrova, E. M., Kazanskaya, O. V., Vasiliev, O. L., Smith, M. W. and Zaraisky, A. G. (1999). The homeobox gene, Xanf-1, can control both neural differentiation and patterning in the presumptive anterior neurectoderm of the Xenopus laevis embryo. *Development* **126**, 4513-4523.

Ermakova, G. V., Solovieva, E. A., Martynova, N. Y. and Zaraisky, A. G. (2007). The homeodomain factor Xanf represses expression of genes in the presumptive rostral forebrain that specify more caudal brain regions. *Dev. Biol.* **307**, 483-497.

Felix, D. A. and Aboobaker, A. A. (2010). The TALE class homeobox gene Smed-prep defines the anterior compartment for head regeneration. *PLoS Genet.* **6**, e1000915.

Fredieu, J. R., Cui, Y., Maier, D., Danilchik, M. V. and Christian, J. L. (1997). Xwnt-8 and lithium can act upon either dorsal mesodermal or neurectodermal cells to cause a loss of forebrain in Xenopus embryos. *Dev. Biol.* **186**, 100-114.

Galceran, J., Farinas, I., Depew, M. J., Clevers, H. and Grosschedl, R. (1999). Wnt3a–/–like phenotype and limb deficiency in Lef1(–/–)Tcf1(–/–) mice. *Genes Dev.* **13**, 709-717.

Garaventa, A., Bellagamba, O., Lo Piccolo, M. S., Milanaccio, C., Lanino, E., Bertolazzi, L., Villavecchia, G. P., Cabria, M., Scopinaro, G., Claudiani, F. et al. (1999). 131I-metaiodobenzylguanidine (131I-MIBG) therapy for residual neuroblastoma: a mono-institutional experience with 43 patients. *Br. J. Cancer* **81**, 1378-1384.

Gaston-Massuet, C., Andoniadou, C. L., Signore, M., Sajedi, E., Bird, S., Turner, J. M. and Martinez-Barbera, J. P. (2008). Genetic interaction between the homeobox transcription factors HESX1 and SIX3 is required for normal pituitary development. *Dev. Biol.* **324**, 322-333.

Glinka, A., Wu, W., Onichtchouk, D., Blumenstock, C. and Niehrs, C. (1997). Head induction by simultaneous repression of Bmp and Wnt signalling in Xenopus. *Nature* **389**, 517-519.

Haegel, H., Larue, L., Ohsugi, M., Fedorov, L., Herrenknecht, K. and Kemler, R. (1995). Lack of beta-catenin affects mouse development at gastrulation. *Development* **121**, 3529-3537.

Heisenberg, C. P., Houart, C., Take-Uchi, M., Rauch, G. J., Young, N., Coutinho, P., Masai, I., Caneparo, L., Concha, M. L., Geisler, R. et al. (2001). A mutation in the Gsk3-binding domain of zebrafish Masterblind/Axin1 leads to a fate transformation of telencephalon and eyes to diencephalon. *Genes Dev.* **15**, 1427-1434.

Houart, C., Caneparo, L., Heisenberg, C., Barth, K., Take-Uchi, M. and Wilson, S. (2002). Establishment of the telencephalon during gastrulation by local antagonism of Wnt signaling. *Neuron* **35**, 255-265.

Houston, D. W., Kofron, M., Resnik, E., Langland, R., Destree, O., Wylie, C. and Heasman, J. (2002). Repression of organizer genes in dorsal and ventral Xenopus cells mediated by maternal XTcf3. *Development* **129**, 4015-4025.

Ivanova, A., Signore, M., Caro, N., Greene, N. D., Copp, A. J. and Martinez-Barbera, J. P. (2005). In vivo genetic ablation by Cre-mediated expression of diphtheria toxin fragment A. *Genesis* **43**, 129-135.

Junghans, D., Hack, I., Frotscher, M., Taylor, V. and Kemler, R. (2005). Beta-catenin-mediated cell-adhesion is vital for embryonic forebrain development. *Dev. Dyn.* **233**, 528-539.

Kazanskaya, O., Glinka, A. and Niehrs, C. (2000). The role of Xenopus dickkopf1 in prechordal plate specification and neural patterning. *Development* **127**, 4981-4992.

Kazanskaya, O. V., Severtzova, E. A., Barth, K. A., Ermakova, G. V., Lukyanov, S. A., Benyumov, A. O., Pannese, M., Boncinelli, E., Wilson, S. W. and Zaraisky, A. G. (1997). Anf: a novel class of vertebrate homeobox genes expressed at the anterior end of the main embryonic axis. *Gene* **200**, 25-34.

Kelberman, D., Rizzoti, K., Lovell-Badge, R., Robinson, I. C. A. F. and Dattani, M. (2009). Genetic regulation of pituitary gland development in human and mouse. *Endocr. Rev.* **30**, 790-829.

Kim, C. H., Oda, T., Itoh, M., Jiang, D., Artinger, K. B., Chandrasekharappa, S. C., Driever, W. and Chitnis, A. B. (2000). Repressor activity of Headless/Tcf3 is essential for vertebrate head formation. *Nature* **407**, 913-916.

Kimmel, C. B., Ballard, W. W., Kimmel, S. R., Ullman, B. and Schilling, T. F. (1995). Stages of embryonic development of the zebrafish. *Dev. Dyn.* **203**, 253-310.

Kimura, C., Yoshinaga, K., Tian, E., Suzuki, M., Aizawa, S. and Matsuo, I. (2000). Visceral endoderm mediates forebrain development by suppressing posteriorizing signals. *Dev. Biol.* **225**, 304-321.

Kudoh, T., Wilson, S. W. and Dawid, I. B. (2002). Distinct roles for Fgf, Wnt and retinoic acid in posteriorizing the neural ectoderm. *Development* **129**, 4335-4346.

Lagutin, O. V., Zhu, C. C., Kobayashi, D., Topczewski, J., Shimamura, K., Puelles, L., Russell, H. R., McKinnon, P. J., Solnica-Krezel, L. and Oliver, G. (2003). Six3 repression of Wnt signaling in the anterior neuroectoderm is essential for vertebrate forebrain development. *Genes Dev.* **17**, 368-379.

Maretto, S., Cordenonsi, M., Dupont, S., Braghetta, P., Broccoli, V., Hassan, A. B., Volpin, D., Bressan, G. M. and Piccolo, S. (2003). Mapping Wnt/beta-catenin signaling during mouse development and in colorectal tumors. *Proc. Natl. Acad. Sci. USA* **100**, 3299-3304.

Martinez-Barbera, J. P., Rodriguez, T. A. and Beddington, R. S. (2000). The homeobox gene Hesx1 is required in the anterior neural ectoderm for normal forebrain formation. *Dev. Biol.* **223**, 422-430.
Merrill, B. J., Pasolli, H. A., Polak, L., Rendl, M., Garcia-Garcia, M. J., Anderson, K. V. and Fuchs, E. (2004). Tcf3: a transcriptional regulator of axis induction in the early embryo. *Development* **131**, 263-274.
Meyers, E. N., Lewandoski, M. and Martin, G. R. (1998). An Fgf8 mutant allelic series generated by Cre- and Flp-mediated recombination. *Nat. Genet.* **18**, 136-141.
Nguyen, H., Merrill, B. J., Polak, L., Nikolova, M., Rendl, M., Shaver, T. M., Pasolli, H. A. and Fuchs, E. (2009). Tcf3 and Tcf4 are essential for long-term homeostasis of skin epithelia. *Nat. Genet.* **41**, 1068-1075.
Paek, H., Hwang, J. Y., Zukin, R. S. and Hebert, J. M. (2011). beta-Catenin-dependent FGF signaling sustains cell survival in the anterior embryonic head by countering Smad4. *Dev. Cell* **20**, 689-699.
Perea-Gomez, A., Rhinn, M. and Ang, S. L. (2001). Role of the anterior visceral endoderm in restricting posterior signals in the mouse embryo. *Int. J. Dev. Biol.* **45**, 311-320.
Piccolo, S., Agius, E., Leyns, L., Bhattacharyya, S., Grunz, H., Bouwmeester, T. and De Robertis, E. M. (1999). The head inducer Cerberus is a multifunctional antagonist of Nodal, BMP and Wnt signals. *Nature* **397**, 707-710.
Rodriguez, C. I., Buchholz, F., Galloway, J., Sequerra, R., Kasper, J., Ayala, R., Stewart, A. F. and Dymecki, S. M. (2000). High-efficiency deleter mice show that FLPe is an alternative to Cre-loxP. *Nat. Genet.* **25**, 139-140.
Sajedi, E., Gaston-Massuet, C., Signore, M., Andoniadou, C. L., Kelberman, D., Castro, S., Etchevers, H. C., Gerrelli, D., Dattani, M. T. and Martinez-Barbera, J. P. (2008). Analysis of mouse models carrying the I26T and R160C substitutions in the transcriptional repressor HESX1 as models for septo-optic dysplasia and hypopituitarism. *Dis. Model. Mech.* **1**, 241-254.
Satoh, K., Kasai, M., Ishidao, T., Tago, K., Ohwada, S., Hasegawa, Y., Senda, T., Takada, S., Nada, S., Nakamura, T. et al. (2004). Anteriorization of neural fate by inhibitor of beta-catenin and T cell factor (ICAT), a negative regulator of Wnt signaling. *Proc. Natl. Acad. Sci. USA* **101**, 8017-8021.
Shimamura, K. and Rubenstein, J. L. (1997). Inductive interactions direct early regionalization of the mouse forebrain. *Development* **124**, 2709-2718.
Spieler, D., Baumer, N., Stebler, J., Koprunner, M., Reichman-Fried, M., Teichmann, U., Raz, E., Kessel, M. and Wittler, L. (2004). Involvement of Pax6 and Otx2 in the forebrain-specific regulation of the vertebrate homeobox gene ANF/Hesx1. *Dev. Biol.* **269**, 567-579.
Srinivas, S., Watanabe, T., Lin, C. S., William, C. M., Tanabe, Y., Jessell, T. M. and Costantini, F. (2001). Cre reporter strains produced by targeted insertion of EYFP and ECFP into the ROSA26 locus. *BMC Dev. Biol.* **1**, 4.
Thomas, P. and Beddington, R. (1996). Anterior primitive endoderm may be responsible for patterning the anterior neural plate in the mouse embryo. *Curr. Biol.* **6**, 1487-1496.
van Amerongen, R. and Nusse, R. (2009). Towards an integrated view of Wnt signaling in development. *Development* **136**, 3205-3214.
van de Water, S., van de Wetering, M., Joore, J., Esseling, J., Bink, R., Clevers, H. and Zivkovic, D. (2001). Ectopic Wnt signal determines the eyeless phenotype of zebrafish masterblind mutant. *Development* **128**, 3877-3888.
Wang, Y., Song, L. and Zhou, C. (2010). The canonical Wnt/ss-catenin signaling pathway regulates Fgf signaling for early facial development. *Dev. Biol.* **349**, 250-260.
Weidinger, G., Thorpe, C. J., Wuennenberg-Stapleton, K., Ngai, J. and Moon, R. T. (2005). The Sp1-related transcription factors sp5 and sp5-like act downstream of Wnt/beta-catenin signaling in mesoderm and neuroectoderm patterning. *Curr. Biol.* **15**, 489-500.
Wilson, S. W. and Houart, C. (2004). Early steps in the development of the forebrain. *Dev. Cell* **6**, 167-181.
Yamamoto, A., Nagano, T., Takehara, S., Hibi, M. and Aizawa, S. (2005). Shisa promotes head formation through the inhibition of receptor protein maturation for the caudalizing factors, Wnt and FGF. *Cell* **120**, 223-235.